Cancer Management and Research

Elevate Series

Open Access Full Text Article

ORIGINAL RESEARCH

A Comprehensive Study of Part-Solid Lung Adenocarcinoma with Lymph Node Metastasis: Clinical, Pathological, and Radiological Perspectives

Ziya Zhao[1,*], Hui Gan[2,*], Bin-jie Fu[1], Wangjia Li[1], Fajin Lv[1], Zhigang Chu[1]

[1]Department of Radiology, The First Affiliated Hospital of Chongqing Medical University, Chongqing, 400016, People's Republic of China; [2]Department of Radiology, The Second Affiliated Hospital of Army Medical University, Chongqing, 400016, People's Republic of China

*These authors contributed equally to this work

Correspondence: Zhigang Chu; Fajin Lv, Department of Radiology, The First Affiliated Hospital of Chongqing Medical University, 1# Youyi Road, Yuanjiagang, Yuzhong District, Chongqing, 400016, People's Republic of China, Tel +86 23 89012302, Fax +86 23 68811487, Email chuzg0815@163.com; fajinlv@163.com

Purpose: Compared to solid lung adenocarcinomas (LUADs), part-solid LUADs rarely exhibit lymph node metastasis (LNM) and generally have a favorable prognosis. This study aims to comprehensively investigate the clinical, pathological, and CT characteristics of part-solid LUADs with LNM.

Patients and Methods: This study collected 70 pathologically confirmed part-solid LUADs at two centers, including 35 cases with LNM and 35 matched cases without LNM based on size, CT pattern, and pathological subtype. Their clinical, pathological, and CT features were comprehensively analyzed and compared to identify the characteristics of part-solid LUADs associated with a high risk of LNM.

Results: Among the 3,457 IACs manifested as part-solid lesions, a total of 35 (1.01%) cases were found to be associated with LNMs. Clinically, patients with and without LNM were similar. Pathologically, lesions exhibiting predominant micropapillary/solid pattern (11.4% vs 0.0%), and containing micropapillary (48.6% vs 25.7%) or any high-grade histological pattern were all more common in part-solid LUADs with LNM than in those without (each $P < 0.05$). Radiologically, solid components located at the tumor margins or distributed in a scattered manner (odds ratio [OR] = 4.048, $P = 0.038$) and consolidation-to-tumor ratio (CTR) > 57.2% (area) (OR = 45.649, $P = 0.041$) were independent predictors of LNM, with an area under the curve of this model being 0.881, sensitivity of 97%, and specificity of 77.1% ($P < 0.001$).

Conclusion: LNM in part-solid LUADs is more prevalent in IACs with high-grade patterns, particularly the micropapillary pattern, with these lesions presenting as part-solid lesions that often have a larger CTR or distinct distribution of solid components.

Keywords: lymphatic metastasis, lung neoplasms, adenocarcinoma of lung, tomography, X-ray computed

Introduction

Currently, lung cancer is one of the leading causes of cancer incidence and mortality, with lung adenocarcinoma (LUAD) being the most common pathological subtype.[1] With the widespread use of low-dose computed tomography (LDCT), the detection rate of ground-glass opacity featured LUADs (GGO-LUADs) has significantly increased.[2] Studies have shown that even in invasive lung adenocarcinomas (IACs), part-solid LUADs have a favorable prognosis compared to solid ones due to their lower aggressiveness and rates of lymph node metastasis (LNM).[3–5] Therefore, they should be treated based on their aggressiveness.

LNM is a significant risk factor for prognosis in patients with early-stage LUAD.[6] A previous study reported that the incidence of LNM in pure ground-glass nodules (pGGNs) is nearly 0%, while that in part-solid nodules (PSNs) is approximately 3.8%; and it is less than 1% when the consolidation-to-tumor (CTR) ratio is below 0.5, whereas it rises to about 5% when the CTR is between 0.5 and 1.[7] This indicates that a minority of part-solid LUADs can also present with

Received: 14 February 2025
Accepted: 20 May 2025
Published: 26 May 2025

LNM. Therefore, lesions with a high risk of LNM warrant special attention and preoperative assessment of the likelihood of LNM in part-solid LUADs is necessary.

Some investigators[8] analyzed 855 of solid and GGO-featured non-small cell lung cancer and found that the incidence of LNM was 7.5%. They identified age, carcinoembryonic antigen (CEA) levels, tumor size, and the CTR as independent predictors of LNM. Similarly, one study[9] conducted a retrospective analysis 651 of solid and GGO LUADs, and identified part or pure solid appearance, elevated CEA levels (>5 ng/dL), and specific histological patterns as predictors of LNM. Notably, only 9 PSNs (3.1%) in them were found to have LNM. Furthermore, a model has been developed to predict LNM in early-stage solid and part-solid LUADs and discovered that age, serum amyloid A (SA), CA125, mucin composition, CK5/6, and napsin-A were important risk factors associated with LNM, which demonstrated high predictive performance.[10]

Although these studies revealed the potential risk factors for predicting LNM, they are all single-center investigations that do not exclusively focus on part-solid LUADs, and they include relatively few samples of part-solid LUADs with LNM. Furthermore, different studies have identified varying predictors, the applicability of the current research findings still requires further validation.

In this study, we conducted a two-center retrospective analysis to comprehensively analyze and compare the clinical, pathological and radiological characteristics of part-solid LUADs with and without LNM in order to identify the features associated with a high risk of LNM.

Materials and Methods

This study conformed to the Declaration of Helsinki on Human Research Ethics standards and was approved by the Institutional Review Board of the First Affiliated Hospital of Chongqing Medical University (No. 2019–062, No. 2025–118-01). The requirement for informed consent was waived because of the retrospective nature of the study. And we confirmed that the data was anonymized or maintained with confidentiality.

Patients

This study retrospectively collected data from patients who underwent pulmonary lesion resection at center 1 from January 2012 to November 2023 and at center 2 from June 2014 to June 2024. A thoracic radiologist who has three years of post-training experience and a senior radiologist, manually reviewed the PACS (Carestream Vue; Carestream, Rochester, NY, USA) and pathological results for these patients.

The inclusion criteria included: (1) patients with a pathological diagnosis of LUAD following surgical resection; (2) the interval between chest CT examination and operation was less than 1 month. The exclusion criteria included: (1) CT images with artifacts affecting assessment; (2) without complete clinical or CT data; and (3) manifesting as solid lesions on CT images. Seventy-two with severe artifacts on CT images affecting the evaluation and 1072 with incomplete clinical or CT data were excluded. Subsequently, 16,385 LUADs were enrolled, including 3,274 adenocarcinomas in situ (AIS), 3,987 minimally invasive adenocarcinomas (MIAs), and 9,124 invasive lung adenocarcinomas (IACs). Of these, pathologically confirmed LNM occurred in 1288 of IACs. And 55 of part-solid LUADs with LNM were collected after the exclusion of solid lesions (1233 cases). Pathological slides and CT images were re-evaluated, further excluding synchronous or metachronous multiple lung cancers (20 cases). Ultimately, 35 of part-solid LUADs with LNM (23 from center 1 and 12 from center 2) and 35 size, CT pattern, and pathological subtype matched cases without LNM (All patients without LNM underwent LN dissection, and the extent of dissection was generally comparable to those with LNM) were enrolled as the control group, resulting in a total of 70 cases. The patients selection process is shown in Figure 1.

CT Examinations

Chest CT examinations were performed using one of the following scanners: Discovery CT 750 hD (GE Healthcare, Milwaukee, WI, USA), SOMATOM Definition Flash (Siemens Healthineers, Erlangen, Germany), SOMATOM Perspective (Siemens Healthineers, Erlangen, Germany), and SOMATOM Force (Siemens Healthineers, Erlangen, Germany). All patients were placed in the supine position with the upper limbs elevated and underwent a breath-

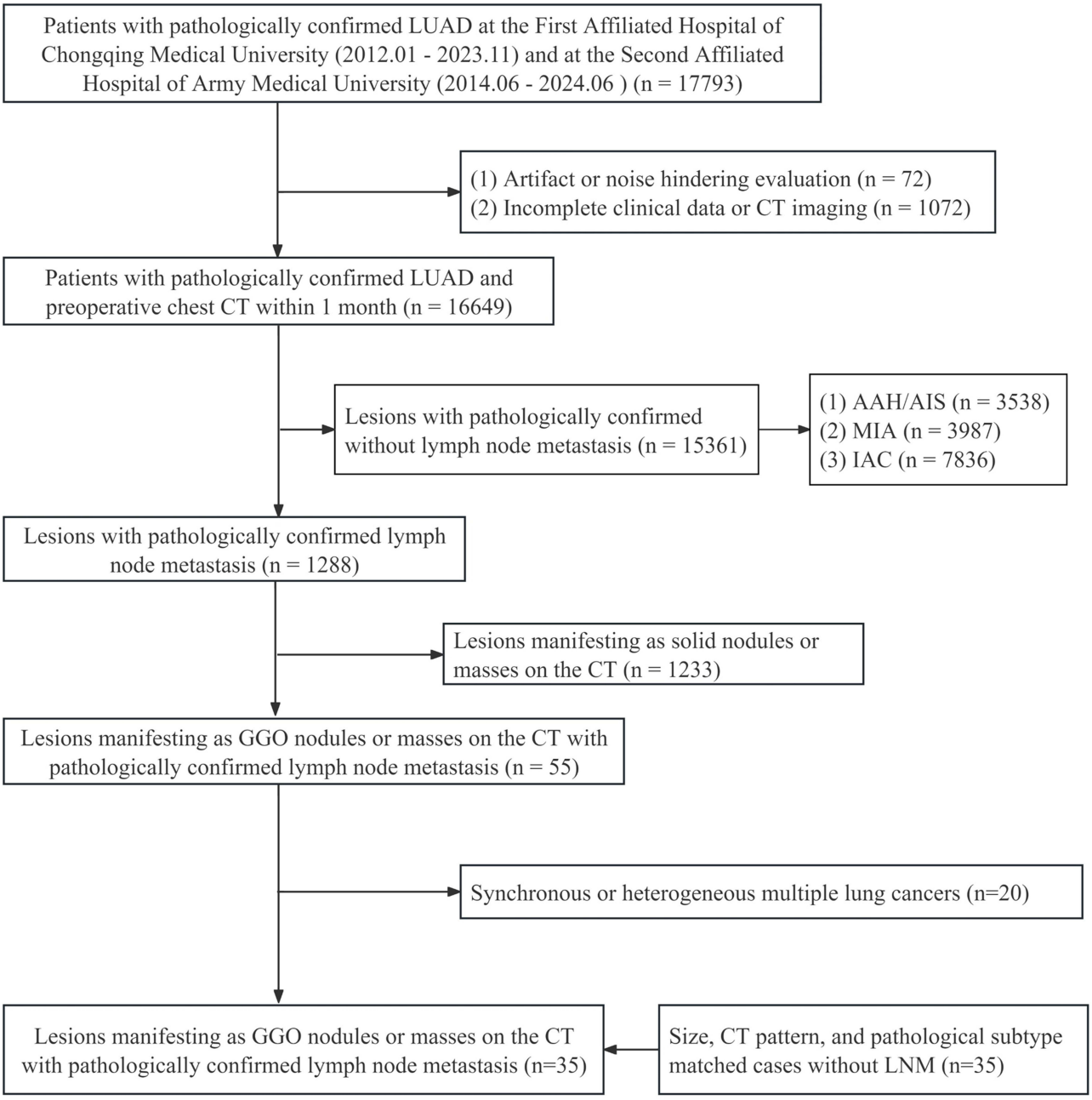

Figure 1 Flowchart of patient selection.

holding exercise before image acquisition. Images were acquired at the end of a deep inspiration during a breath-hold. The scanning range was from the thoracic inlet to the costophrenic angle. Scanning parameters were set as follows: tube voltage, 100–120 kVp; tube current, 50–200 mAs (reference mAs, using the electron tube current auto-adjustment technique); scanning slice thickness and slice spacing, 5 mm; reconstruction slice thickness and spacing, 0.625 (GE scanner) or 1 mm (Siemens scanner); matrix: 512 × 512; rotation time, 0.5–0.6 seconds; spacing, 0.9–1; using iterative reconstruction with a standard-sharpness (GE CT scanners) or medium-sharpness (Siemens CT scanners) algorithm.

Image Interpretation

Unenhanced CT data for all patients were analyzed on a PACS workstation (Carestream Vue PACS) by two experienced chest radiologists using lung windows (window level: −600 hU; window width: 1500 hU), without knowledge of the

https://doi.org/10.2147/CMAR.S520781

pathological results and clinical information. If there was disagreement on the results, consensus was reached after joint discussion.

The following features of the lesions were analyzed based on thin-section CT images: (1) size (average of the longest diameter and vertical diameter on axial CT images); (2) location (right upper lobe, right middle lobe, right lower lobe, left upper lobe, or left lower lobe); (3) shape (round, oval or irregular); (4) boundary (ill-defined or well-defined); (5) lobulation sign, spiculation sign, pleural indentation sign, vacuole sign, air bronchogram sign, and vascular changes; (6) concomitant pneumonia, emphysema or other solid nodules (SNs); (7) distribution of solid components (central distribution, located at the tumor margin, or scattered distribution); (8) CTR: the ratio of the maximum diameter and area of the solid components to the maximum diameter and area of the tumor is measured at the largest section of the tumor; (9) the CT value of solid component (CT_1) and GGO component (CT_2), and difference between CT_1 and CT_2 ($\Delta CT= CT_1 - CT_2$); and (10) determining whether hilar and mediastinal lymph nodes (LNs) enlarged and their stations, and measuring the short diameter of the LNs.

Abnormal intra-nodular vessel was considered present when intra-nodular vascular segments were dilated (ie, diameter of vascular segment greater than that of segments proximal to the vessel's entry into the nodule, or diameter of vascular segment significantly greater than that of other vessels at the same branch level), or distorted (ie, vessel deviated from its normal route).[11] Concerning the distribution of the single solid component, it was classified as central distribution if it was completely surrounded by the GGO component. Conversely, it was considered to be at the tumor margin if it was only partially surrounded by the GGO component. In cases where multiple solid components were present within the tumor, they were regarded as having a scattered distribution. The size of the solid component is defined as its maximum diameter measured in the lung window. CTR (length) is defined as the ratio of the maximum diameter of the solid component to the maximum diameter of the lesion. CTR (area): the ratio of the area of the solid component to the area of tumor (area is automatically measured by the PACS workstation after manually outlining the boundary of solid components and lesions). The CT_1 and CT_2 of lesions were measured separately by drawing region of interest (ROI) (avoiding blood vessels and bronchioles) at the largest section of lesions on the workstation. LN enlargement is defined as a short axis diameter of 10 mm or greater on CT images.[12]

The artificial intelligence (AI) parameters for nodules obtained from the lung AI-assisted diagnosis system (Infer Read CT Lung, InferVision Medical Health, Beijing, China and Deep wise AI Lung Cancer Analysis software, China) are as follows: mean CT value (HU), CTR (thresholds of −250, −300, and −350), sphericity, compactness, tumor volume (mm^3).

Clinical Analysis

Patients clinical data were collected using an electronic medical record system (Winning Health, China; GE Healthcare, China). The patients' clinical information included age, gender, history and family history of malignant tumors, smoking history, and history of lung diseases (chronic obstructive pulmonary disease, bronchial asthma, tuberculosis, or pneumonia). Preoperative hematological parameters included: (1) lymphocytes. (2) tumor markers: carcinoembryonic antigen (CEA), neuron-specific enolase (NSE), pro-gastrin-releasing peptide precursor (pro-GRP), cytokeratin 19 fragments (cybra21-1), and squamous cell carcinoma antigen (SCC). (3) inflammatory markers: serum complement C1q and derived neutrophil-lymphocyte ratio (NLR), platelet-lymphocyte ratio (PLR), monocyte-lymphocyte ratio (MLR), derived neutrophil-lymphocyte ratio (dNLR), neutrophil-lymphocyte and platelet ratio (NLPR), systemic inflammatory response syndrome (SIRS), aggregate index of systemic inflammation (AISI), and systemic inflammatory index (SII).[10]

Histopathologic Analysis

Formalin-fixed paraffin-embedded tissues were sectioned and then stained with hematoxylin and eosin and Alcian Blue-Periodic Acid-Schiff (AB-PAS) method. The initial diagnosis was made by a junior pathologist and the final diagnosis was confirmed by a senior pathologist. The 2011 classification system by IASLC/ATS/ERS classified LUAD into five distinct histological patterns: lepidic, acinar, papillary, micropapillary, and solid,[13] and the pathological subtypes of LUAD include AIS, MIA and IAC. According to the latest IASLC grading system, IAC is classified into three grades based on the proportions of histological patterns: well differentiated (lepidic-predominant with high-grade histological

patterns < 20%), moderately differentiated (acinar or papillary-predominant with high-grade histological patterns < 20%), and poorly differentiated (any pattern with high-grade histological patterns > 20%). High-grade histological patterns include solid, micropapillary, and sieve or complex glandular patterns.[14]

LNM was confirmed by postoperative pathological sections. According to the 8th edition of the TNM lung cancer classification,[15] superior mediastinal LN (SMLN) were defined as stations 2R, 3 and 4R for right lung cancers, and stations 4L, 5 and 6 for left lung cancers. Inferior mediastinal LN (IMLN) were defined as stations 7–9. Skip metastasis is typically defined as the presence of mediastinal LNM without any involvement of N1 LNs on the same side.

Statistical Analysis

All data in this study were statistically analyzed using SPSS (version 27.0, IBM, New York, USA). The intraclass correlation coefficient (ICC) and Cohen kappa coefficient were used to assess the interobserver agreement of continuous and categorical variables, respectively.[16] The patients' clinical, pathological and radiological features of lesions were statistically analyzed, with continuous variables expressed as mean ± standard deviation (SD) and categorical variables expressed as counts and percentages. Continuous variables were tested for normality, and variables that did not conform to normal distribution were expressed as M (P25, P75). Mann–Whitney U rank sum test was used to analyze differences in continuous variables. Pearson's chi-square test or Fisher's exact test was used to analyze differences in categorical variables. After completing univariate analysis, variables with statistically significant differences were included in further logistic regression analysis to identify independent predictors associated with LNM. Due to the small sample size, we use min-max normalization for enhancing the stability of the model. Receiver operating characteristic curves (ROC) was plotted and the area under the curve (AUC) was calculated, with the optimal cut-off value determined to be the point closest to the upper left corner of the ROC curve. The factor was considered a statistically significant difference if $p < 0.05$.

Results

Occurrence of LNM in Part-Solid LUADs

Among the 3,931 GGO featured IACs, 3,457 (87.9%) were part-solid lesions, and 474 (12.1%) were pure ground-glass lesions. Part-solid LUADs with LNM was absent in pure ground-glass lesions. Among the 3,457 IACs manifested as part-solid lesions, a total of 35 (1.01%) cases were found to be associated with LNMs.

Clinical Characteristics and Laboratory Examinations of Part-Solid LUADs with LNM

The clinical characteristics and laboratory examinations are summarized in Table 1. The levels of CEA, NLR, and dNLR were significantly higher in part-solid LUADs with LNM than those without (each $P < 0.05$). Conversely, the levels of NSE, CA19-9, SCC-Ag, and lymphocyte counts were higher in part-solid LUADs without LNM than in those with LNM (each $P < 0.05$). Nevertheless, all these indicators remained within normal limits in both groups.

CT Characteristics of Part-Solid LUADs with LNM

The CT characteristics of part-solid LUADs with and without LNM are summarized in Table 2. Compared to part-solid LUADs without LNM, those with LNM are more likely to exhibit solid components located at the tumor margin or scattered throughout the tumor (Figures 2–4) and have concomitant SNs (each $P < 0.05$). Furthermore, the compactness, mean CT value, CT_2, and CTR (length, area, and density based on different thresholds) were all significantly higher in part-solid LUADs with LNM compared to those without (each $P < 0.001$).

Interobserver Agreement

Table S1 summarizes the interobserver agreement for the CT features of the lesions. For continuous variables, inter-observer agreement was good (ICC = 0.854–0.870). For categorical variables, inter-observer agreement was substantial or almost perfect (κ = 0.799–0.902).

Table 1 Patients' Clinical Characteristics and Laboratory Examinations

	Part-Solid LUADs with LNM (n = 35)	Part-Solid LUADs without LNM (n = 35)	*P*-Value
Gender (male)	20 (52.6)	18 (47.4)	0.65
Age (years)	59.14 ± 9.80	61.51 ± 8.34	0.279
Smoking history	18 (47.4)	13 (34.2)	0.24
History or family history of malignant tumors	3 (7.6)	3 (7.9)	1.00
Previous history of lung disease	0 (0.0)	1 (2.6)	0.24
NSE (0–16.3 ng/mL)	9.90 (8.70, 11.30)	11.20 (10.60, 12.30)	0.004
CEA (0.2–10.0 ng/mL)	3.00 (2.00, 7.19)	2.10 (1.50, 3.00)	0.015
CYFRA21-1 (0.0–3.3 ng/mL)	2.00 (1.50, 2.88)	2.40 (2.10, 3.20)	0.045
proGRP (25.3–77.8 pg/mL)	46.79 ± 15.18	50.05 ± 16.13	0.387
SCC-Ag (0.0–1.5 ng/mL)	0.80 (0.60, 1.10)	1.20 (0.80, 1.40)	0.016
Lymphocyte (1.10–3.20,10^9/L)	1.60 (1.21, 1.78)	1.88 (1.44, 2.26)	0.008
NLR	2.33 (1.82, 2.82)	1.76 (1.45, 2.22)	0.015
PLR	127.33 (97.25, 158.77)	110.71 (79.35, 151.06)	0.499
MLR	0.24 (0.19, 0.34)	0.22 (0.18, 0.28)	0.344
dNLR	1.68 (1.27, 1.96)	1.35 (1.01, 1.61)	0.024
NLPR	0.01 (0.01, 0.02)	0.01 (0.01, 0.01)	0.054
SIRI	0.80 (0.57, 1.29)	0.78 (0.51, 0.95)	0.353
AISI	136.01 (100.51, 243.07)	165.62 (103.93, 243.17)	0.668
SII	415.59 (279.84, 546.00)	385.16 (297.97, 527.91)	0.609

Notes: Continuous data are shown as or mean ± standard deviation or median (interquartile range, IQR), and categorical data as number (percentage).

Abbreviations: NSE, Neuron-specific enolase; CEA, Carcinoembryonic antigen; proGRP, Progastrin releasing peptide; SCC-Ag, Squamous cell carcinoma antigen; CYFRA21-1, Cytokeratin 19 fragment; NLR, neutrophil–lymphocyte ratio; PLR, platelet-lymphocyte ratio; MLR, monocyte-lymphocyte ratio; dNLR, derived neutrophil-to-lymphocyte ratio; NLPR, neutrophil to lymphocyte and platelet ratio; SIRI, systemic inflammatory response syndrome; AISI, aggregate index of systemic inflammation; SII, systemic inflammation index.

Table 2 The CT Characteristics of Lesions with and Without Lymph Node Metastasis

	Part-Solid LUADs with LNM (n = 35)	Part-Solid LUADs without LNM (n = 35)	*P*-Value
Size	21.74 ± 8.01	21.74 ± 8.01	-
Boundary			
Well-defined	18 (51.4)	24 (68.6)	0.143
Ill-defined	17 (48.6)	11 (31.4)	
Shape			
Round/oval	4 (11.4)	4 (11.4)	1
Irregular	31 (88.6)	31 (88.6)	
Lobulation sign	34 (97.1)	31 (88.6)	0.151
Spiculation sign	22 (62.9)	9 (25.7)	0.002
Pleural indentation sign	25 (71.4)	24 (68.6)	0.794
Vacuole sign	22 (62.9)	22 (62.9)	1
Air bronchogram sign	16 (45.7)	20 (57.1)	0.339
Vascular sign	9 (25.7)	14 (40.0)	0.203
Location			0.636
LUL	10 (28.6)	7 (20.0)	
LLL	5 (14.3)	5 (14.3)	
RUL	11 (31.4)	16 (45.7)	
RML	0 (0)	0 (0)	
RLL	9 (25.7)	7 (20.0)	

(*Continued*)

Table 2 (Continued).

	Part-Solid LUADs with LNM (n = 35)	Part-Solid LUADs without LNM (n = 35)	*P*-Value
Distribution of solid components			< 0.001
Central distribution	8 (22.9)	23 (65.7)	
Located at the tumor margin or scattered distribution	27 (77.1)	12 (34.3)	
CTR (length)	0.67 ± 0.14	0.44 ± 0.19	< 0.001
CTR (area)	0.49 (0.36, 0.57)	0.15 (0.08, 0.39)	< 0.001
CT_1 (HU) (%)	29 (8.00, 38.00)	10 (−12.00, 33.00)	0.092
CT_2 (HU) (%)	−463.87 ± 106.88	−523.00 ± 120.87	0.034
ΔCT (HU) (%)	475.90 ± 100.07	520.97 ± 125.46	0.101
Tumor volume (mm^3)	5472.0 (2612.9, 6072.1)	4134.8 (1859.0, 6980.7)	0.401
Mean CT value (HU)	−230.7 (−256.0, −170.0)	−384.0 (−525.0, −275.0)	< 0.001
CTR (250) (%)	45.3 (35.5, 56.6)	20.28 (9.28, 41.25)	< 0.001
CTR (300) (%)	51.53 ± 18.40	32.12 ± 21.68	< 0.001
CTR (350) (%)	57.17 ± 19.03	38.40 ± 23.75	< 0.001
Compactness	0.04 (0.031, 0.50)	0.03 (0.029, 0.035)	0.015
Sphericity	0.76 ± 0.10	0.73 ± 0.07	0.134
Concomitant emphysema	7 (20.0)	6 (17.1)	0.759
Concomitant pneumonia	7 (20.0)	3 (8.6)	0.172
Concomitant SNs	19 (54.3)	0 (0)	< 0.001

Notes: Continuous data are shown as or mean ± standard deviation or median (interquartile range, IQR), and categorical data as number (percentage). -: The sizes of the lesions in the two groups are consistent, and no statistical analysis has been conducted.
Abbreviations: CT_1, the maximal CT value of the solid component; CT_2, the maximal CT value of the GGO; ΔCT, difference between CT values of solid and GGO component; LLL, left lower lobe; LUL, left upper lobe; RLL, right lower lobe; RML, right middle lobe; RUL, right upper lobe; CTR, consolidation tumor ratio; SN, solid nodule.

Logistic Regression Analysis of CT Features for Part-Solid LUADs

The CT features that independently predicted LNM as determined by logistic regression are summarized in Table 3. The solid components located at the tumor margin or scattered distribution (OR = 4.048, P = 0.038) and CTR (area) (OR = 45.649, P = 0.041) were independent predictors of LNM for IACs manifested as part-solid lesions. The sensitivity,

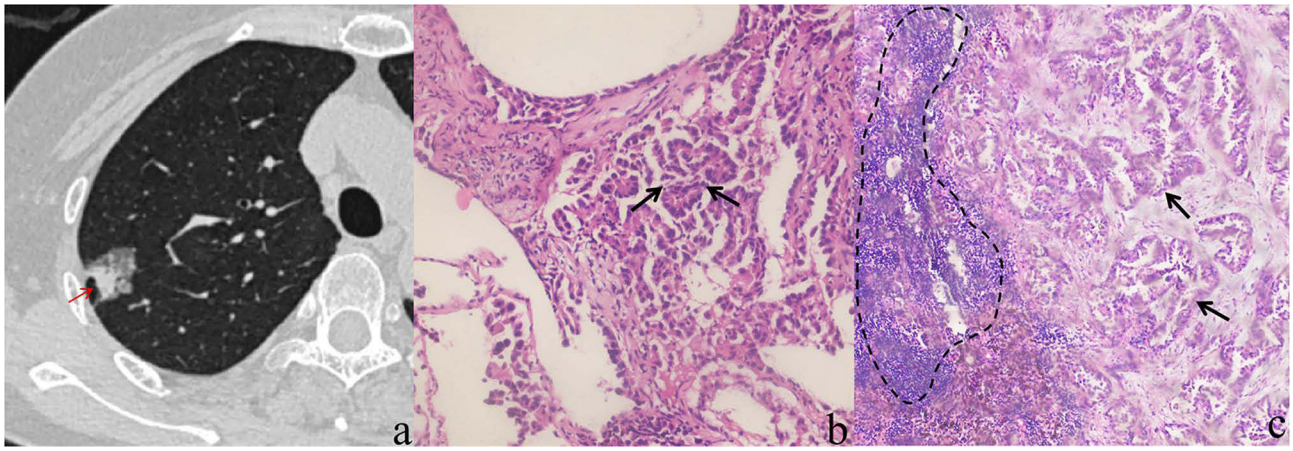

Figure 2 A 66-year-old female with pathologically confirmed moderately differentiated IAC with LNM. (**a**) A transverse thin-section non-enhanced CT image shows a large (20 mm), lobulated, and well-defined PSN located in the right upper lobe, with the solid component (red arrow) located at the tumor margin. (**b**) Photomicrograph of histopathologic specimen (HE, ×20) shows an invasive micropapillary pattern (black arrows) in the lesion, constituted by clusters of micropapillary cells suspended in the glandular cavity without a fibrovascular core. (**c**) Photomicrograph of LN specimen (HE, ×10) shows cancerous tissue invasion (black arrows). Partial stromal necrosis or fibrosis can be observed, with a slight infiltration of inflammatory cells (delineated by dotted lines).
Abbreviations: PSN, part-solid nodule; IAC, invasive lung adenocarcinomas.

https://doi.org/10.2147/CMAR.S520781

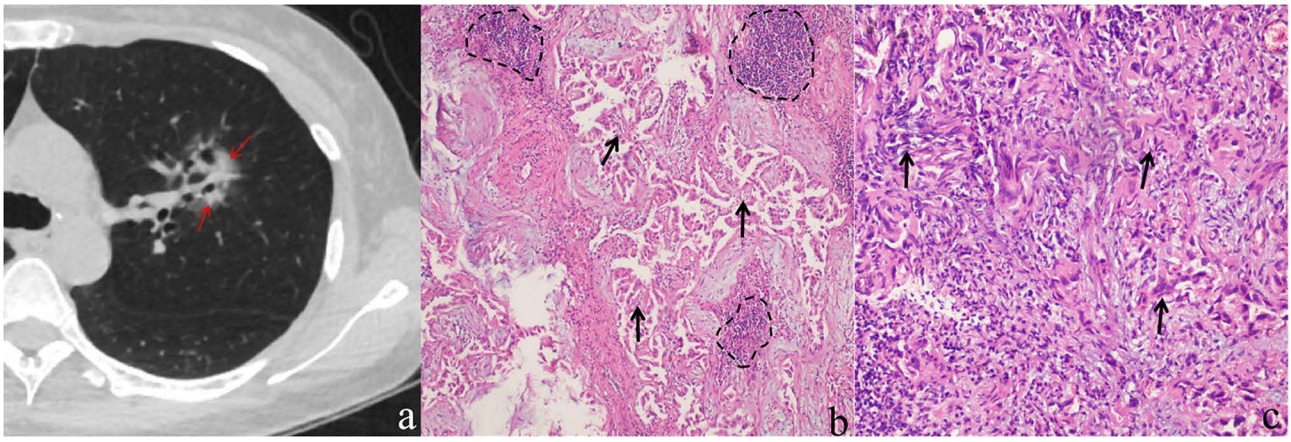

Figure 3 A 48-year-old male with pathologically confirmed poorly differentiated IAC with LNM. (**a**) A transverse thin-section non-enhanced CT image shows a large (29 mm), spiculated, and ill-defined PSN located in the left upper lobe, with the solid components (red arrows) scattered within the nodule. (**b**). Photomicrograph of histopathologic specimen (HE, ×10) shows an shows an invasive micropapillary pattern (black arrows) in the lesion, and the surrounding stroma shows fibrosis and slight infiltration of inflammatory cells (delineated by dotted lines). (**c**) Photomicrograph of the LN specimen (HE, ×20) shows cancerous tissue invasion (black arrows) with slight infiltration of inflammatory cells.
Abbreviations: PSN, part-solid nodule; IAC, invasive lung adenocarcinomas.

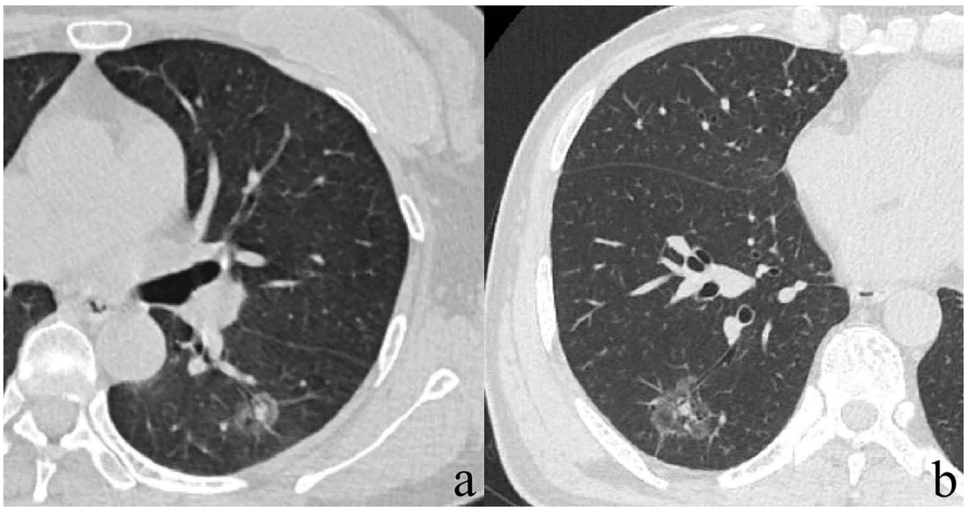

Figure 4 (**a**) A 54-year-old male of pathologically confirmed moderately differentiated IAC without LNM. A transverse thin-section non-enhanced CT image shows a large (14 mm), well-defined PSN located in the left lower lobe, with the solid component completely surrounded. (**b**) A 60-year-old male of pathologically confirmed moderately differentiated IAC without LNM. A transverse thin-section non-enhanced CT image shows a large (25 mm), spiculated, well-defined PSN located in the right lower lobe, with the solid components completely surrounded.

specificity and area under the curve (AUC) of the model were 97.0%, 77.1% and 0.881 (95% CI: 0.800–0.962), respectively ($P < 0.001$) (Figure S1).

Pathological Features of Part-Solid LUADs with LNM

The pathological features of part-solid LUADs with and without LNM are summarized in Table 4. Lesions exhibiting a predominant micropapillary/solid pattern (11.4% vs 0.0%), and containing micropapillary pattern (48.6% vs 25.7%) or any high-grade histological pattern (57.1% vs 25.7%) were all significantly more common in part-solid LUADs with LNM than those without (each $P < 0.05$).

Of the 35 lesions with LNM, 9 (25.7%) were poorly differentiated, 22 (62.9%) were moderately differentiated, and 4 (11.4%) were well differentiated. In contrast, among the 35 lesions without LNM, none (0%) were poorly differentiated,

Table 3 Multi-Variable Binary Logistic Regression Analysis of CT Characteristics

Variables	Odds Ratio	95% CI		*P*-Value
		Lower Limit	Upper Limit	
Spiculation	2.489	0.626	9.899	0.196
CTR (area)	45.649	1.160	1796.266	0.041
Solid components located at the tumor margin or scattered distribution	4.048	1.083	15.135	0.038
CT_2	1	0.993	1.007	0.997
Mean CT value	1.004	0.998	1.011	0.208

Notes: Data are reported as values with 95% CI in parentheses.
Abbreviations: CI, confidence interval; CTR, consolidation tumor ratio; GGO, Ground-glass opacity; CT2, the maximal CT value of the GGO.

Table 4 The Pathological Features of Lesions with or Without Lymph Node Metastasis

	Part-Solid LUADs with LNM (n = 35)	Part-Solid LUADs without LNM (n = 35)	*P*-Value
Histological patterns			
Lepidic pattern	21 (60.0)	15 (42.9)	0.151
Acinar pattern	33 (94.3)	35 (100.0)	0.473
Papillary pattern	18 (51.4)	16 (45.7)	0.811
Solid pattern	5 (14.3)	1 (2.9)	0.200
Micropapillary pattern	17 (48.6)	9 (25.7)	0.048
Complex glandular pattern	2 (5.7)	0 (0.0)	0.473
Any high-grade pattern	20 (57.1)	9 (25.7)	0.008
Predominant histological pattern			
Lepidic pattern	5 (14.3)	6 (17.1)	0.743
Acinar/ papillary pattern	26 (74.3)	29 (82.9)	0.382
Solid/ micropapillary pattern	4 (11.4)	0 (0.0)	0.016
Pathological grading			
Poorly differentiated	9 (25.7)	0 (0.0)	< 0.001
Moderately differentiated	22 (62.9)	29 (82.9)	0.06
Well differentiated	4 (11.4)	6 (17.1)	0.495

Notes: Data are expressed as n (%). High-grade pattern include solid, micropapillary, sieve or complex glandular patterns.

29 (82.8%) were moderately differentiated, and 6 (17.1%) were well differentiated. The occurrence of poorly differentiated was significantly higher in cases with LNM than those without ($P < 0.001$).

Location and CT Features of Metastatic LNs

The location and CT features of metastatic LNs is summarized in Table S2. Among the 35 lesions with LNM, a total of 85 stations were involved. Specifically, intrapulmonary and hilar LN, SMLN, and IMLN metastases were 22 (62.9%), 19 (54.3%), and 13 (37.1%), respectively. Single-station LNM occurred in 13 (37.1%), while multi-station LNM occurred in 22 (62.9%). Skip metastases were noted in 13 (37.1%) cases. In 21 cases with tumors located in upper lobes, IMLN metastasis were present in 4 (19.0%), and three (75.0%) of them had no hilar LNM. In 14 patients with tumors located in lower lobes, SMLN metastasis were present in 7 (50.0%), and three (42.9%) of them had no hilar LNM. On CT images, 10 (28.6%) cases exhibited enlarged metastatic LNs, with a mean short axis measurement of 12.04 ± 2.36 (range: 10–16 mm). The enlarged LNs located in the hilum (5, 50%), superior mediastinum (4, 40%), and inferior mediastinum (1, 10%), respectively.

Discussion

This study provides a comprehensive analysis and comparison of the clinical, pathological, and radiological characteristics of part-solid LUADs with LNM. The sample size of part-solid LUADs with LNM in this study is relatively large compared to current literature. Notably, all lesions with LNM were identified in IACs presenting as part-solid lesions, with an incidence of 1.01%. Pathologically, lesions exhibiting predominant micropapillary/solid pattern, and those containing micropapillary or any high-grade histological pattern, were all more prevalent in part-solid LUADs with LNM. Regarding CT features, solid components located at the tumor margins or distributed in a scattered manner, along with a CTR (area) greater than 57.2%, were identified as independent predictors of LNM in part-solid LUADs. For patients with lesions exhibiting indicators of LNM, SLND may be more appropriated because some prone to skip metastasis.

Previous studies have shown that LUADs characterized by predominantly micropapillary or solid patterns are associated with elevated risk of LNM.[17–19] Similarly, this study found that the occurrence of LNM in part-solid LUADs is closely related to the predominance of these histological patterns. Notably, a significant correlation was also identified between LNM and the presence of micropapillary or any high-grade histological patterns, irrespective of whether they were predominant or not. This indicates that even if these patterns constitute only a small portion of the lesion, they may still suggest a poor prognosis, which is consistent with the conclusions of previous research.[20,21] However, some part-solid LUADs without LNM also contained high-grade patterns, this implies that LNM may also be influenced by the rate of disease progression and biological characteristics. Therefore, high-grade patterns should be considered as potential risk factors for LNM rather than definitive determinants. Nonetheless, accurate preoperative identification of these high-grade patterns remains crucial for effective management.

Overall, LNM is uncommon in patients with GGO-LUADs, and its occurrence exhibits considerable variability. It was found that the incidence of LNM in pure GGO lesions was approximately 0%, while for part-solid lesions was around 3.8%, ranging from 0% to 7.9% in different studies. This may be attributed to variations in sample inclusion criteria. In this study, LNM was exclusively observed in IACs presenting as part-solid lesions with an incidence of 1.01%. Previous studies[22,23] have indicated that a significantly higher rate of LNM in part-solid lesions with CTR > 50%. This study also corroborated that lesions with higher risk of LNM when CTR (area) > 57.2%. Additionally, previous studies[24,25] revealed that PSNs with larger, irregular, multiple, scattered and eccentric solid components had a higher probability of malignancy. This study also identified that the distribution of internal solid components related to LNM. The correlation between them may be attributed to the following factors. Firstly, the occurrence and development of solid components located at the tumor margins or distributed in a scattered manner may differ from those found in the central area. Secondly, the marginal and scattered solid components may indicate a higher degree of tumor heterogeneity, which is consistent with our findings that such lesions more frequently contain high-grade histological patterns. Thirdly, compared to central solitary solid component, marginal or scattered solid components are more likely to represent invasive components rather than alveolar collapse or fibrosis. Finally, these marginal invasive components are closer to normal lung tissue, making them more prone to invade adjacent lymphatic vessels, resulting in LNM. However, these hypotheses should be fully validated and warrants further investigation in the further studies. Furthermore, this study noted that some lesions with CTR < 50% still exhibited LNM, particularly those with marginal or scattered distributions of solid components. This finding indicates that the CTR and the distribution of solid components serve as complementary indicators in assessing the risk of LNM. The combination of these two factors enables for a more comprehensive evaluation of the tumor's metastatic potential, thereby providing valuable information for surgical decision-making.

Levels of tumor markers could reflect the nature of tumors. Regarding early-stage LUADs, it was found that CEA and CA125 may be independent risk factors for LNM.[10,26] This study also found that lesions with LNM exhibited slightly higher serum CEA levels, but the difference was not significant. Additionally, several studies have explored the relationship between clinical inflammation indicators and the risk of LNM. Qu et al[27] found that elevated platelet counts were significantly associated with LNM, even when they remained within the reference range. Similarly, Chen et al[28] identified the ratio of lymphocytes to monocytes as an independent risk factor for LNM. In this study, preoperative NLR and dNLR were higher in lesions with LNM than those without, while lymphocyte counts were lower. These indicators

suggest impaired immune function, which typically suppresses tumor cell proliferation and metastatic activity.[29] However, due to the complex interactions among circulating inflammatory cells, these indicators can only partially reflect metastatic risk. It is evident that laboratory examinations alone are insufficient for assessing the risk of LNM in part-solid LUADs, and further research is needed to clarify their relationship.

Currently, the National Comprehensive Cancer Network (NCCN) guidelines[30] recommend systematic LN dissection (SLND) or mediastinal LN sampling (MLNS) (3 of N2 and 1 of N1 LN stations) for early-stage NSCLCs. Zhang et al[31] summarized the LNM regularity of 2,749 patients with invasive NSCLC, and proposed a new selective mediastinal LN dissection strategy for NSCLC. They pointed out that tumors located in the upper lobe of the lung and negative hilar LNs did not require IMLN dissection. However, in this study, the probability of upper lobe lesions affecting the IMLN was 19.0%, and three of them without hilar LNM. This indicated that some lesions exhibit irregular patterns of LNM, including a tendency for skip metastasis, which may be related to the radiological and pathological features of tumors, as well as their distribution. This prompts that MLNS or selective mediastinal LN dissection strategy may not be suitable for all part-solid LUADs, and the part-solid lesions with a high suspicion of LNM may still require SLND. Additionally, a previous study has shown that LN size is not a reliable parameter for assessing metastasis in lung cancers.[32] This study also found that enlarged metastatic LNs are rarely observed in part-solid LUADs, and often present with only mild enlargement. The measurement of LN is usually influenced by many factors. Therefore, determining LNM solely based on the size of LNs on CT images is also unreliable.

There are several limitations in this study that should be acknowledged. Firstly, while this is a retrospective study with a sample size that is relatively larger compared to previous studies, the number of cases with LNM is still relatively small overall, which may affect the stability of the conclusions. Therefore, the new findings in this study should be further verified. Secondly, due to the different surgical and lymphadenectomy methods employed, not all LNs in the patients were sampled, which may introduce some bias in the analysis. Thirdly, in selecting the control group, this study matched participants solely based on the size, CT pattern, and pathological subtype of the lesions, without taking other factors into account. Furthermore, We selected a very limited number of cases from those without LNM to form the control group. These aspects may introduce bias into the study. Finally, the assessment of LNM was limited to IACs manifested as part-solid nodules or masses, so it is essential to assess the invasiveness of lesions before evaluating the possibility of LNM.

In conclusion, LNM is significantly associated with the presence of high-grade histological patterns, particularly the micropapillary pattern, regardless of whether they are predominant. The effectiveness of clinical and laboratory examinations in assessing LNM in part-solid LUADs is limited. Radiologically, LNM was observed exclusively in IACs manifesting as part-solid lesions, with an extremely low incidence of 1.01%. Lesions with solid components located at the tumor margin or scattered distribution, as well as those with a CTR greater than 57.2% had a higher risk of LNM. Although metastasized LNs could be identified on CT images, they often did not show significant enlargement. When a part-solid lesions is suspected to be an IAC, it is essential to evaluate the distribution and proportion of the internal solid components to assess the potential for LNM. For patients with lesions showing indicators of skip metastasis, a systematic lymphadenectomy may be warranted.

Ethical Approval

This study conformed to the Declaration of Helsinki on Human Research Ethics standards and was approved by the Institutional Review Board of the First Affiliated Hospital of Chongqing Medical University (No. 2019-062, No. 2025-118-01). The requirement for informed consent was waived because of the retrospective nature of the study. And we confirmed that the data was anonymized or maintained with confidentiality.

Author Contributions

All authors made a significant contribution to the work reported, whether that is in the conception, study design, execution, acquisition of data, analysis and interpretation, or in all these areas; took part in drafting, revising or critically reviewing the article; gave final approval of the version to be published; have agreed on this journal to which the article has been submitted; and agree to be accountable for all aspects of the work.

Funding

This work was supported by the Project of Chongqing Natural Science Foundation (No.CSTB2024NSCQ-MSX0655), a joint project of Chongqing Municipal Science and Technology Commission and Chongqing Municipal Health Planning Commission (2022MSXM050 and 2022QNXM053), and the Senior Medical Talents Program of Chongqing for Young and Middle-aged from Chongqing Health Commission (to Z.G.C.).

Disclosure

The authors report no conflicts of interest in this work.

References

1. Bray F, Laversanne M, Sung H, et al. Global cancer statistics 2022: GLOBOCAN estimates of incidence and mortality worldwide for 36 cancers in 185 countries. *CA Cancer J Clin*. 2024;74(3):229–263. doi:10.3322/caac.21834
2. de Koning HJ, van der Aalst CM, de Jong PA, et al. Reduced Lung-Cancer Mortality with Volume CT Screening in a Randomized Trial. *N Engl J Med*. 2020;382(6):503–513. doi:10.1056/NEJMoa1911793
3. Sakurai H, Goto Y, Yoh K, et al. Prognostic significance of ground-glass areas within tumours in non-small-cell lung cancer. *Eur J Cardiothorac Surg*. 2024;65(4):158. doi:10.1093/ejcts/ezae158
4. Hattori A, Suzuki K, Takamochi K, et al. Prognostic impact of a ground-glass opacity component in clinical stage IA non-small cell lung cancer. *J Thorac Cardiovasc Surg*. 2021;161(4):1469–1480. doi:10.1016/j.jtcvs.2020.01.107
5. Deng J, Zhao M, Wang T, et al. A modified T categorization for part-solid lesions in Chinese patients with clinical stage I Non-small cell lung cancer. *Lung Cancer*. 2020;145:33–39. doi:10.1016/j.lungcan.2020.04.028
6. Higgins KA, Chino JP, Ready N, et al. Lymphovascular invasion in non-small-cell lung cancer: implications for staging and adjuvant therapy. *J Thorac Oncol*. 2012;7(7):1141–1147. doi:10.1097/JTO.0b013e3182519a42
7. Xu S, He Z, Li X, et al. Lymph Node Metastases in Surgically Resected Solitary Ground-Glass Opacities: a Two-Center Retrospective Cohort Study and Pooled Literature Analysis. *Ann Surg Oncol*. 2023;30(6):3760–3768. doi:10.1245/s10434-023-13235-7
8. Koike T, Koike T, Yamato Y, Yoshiya K, Toyabe S. Predictive risk factors for mediastinal lymph node metastasis in clinical stage IA non-small-cell lung cancer patients. *J Thorac Oncol*. 2012;7(8):1246–1251. doi:10.1097/JTO.0b013e31825871de
9. Ye B, Cheng M, Li W, et al. Predictive factors for lymph node metastasis in clinical stage IA lung adenocarcinoma. *Ann Thorac Surg*. 2014;98(1):217–223. doi:10.1016/j.athoracsur.2014.03.005
10. Xue M, Liu J, Li Z, et al. The role of adenocarcinoma subtypes and immunohistochemistry in predicting lymph node metastasis in early invasive lung adenocarcinoma. *BMC Cancer*. 2024;24(1):139. doi:10.1186/s12885-024-11843-4
11. Fu BJ, Zhang XC, Lv FJ, Chu ZG. Potential Role of Intrapulmonary Concomitant Lesions in Differentiating Non-Neoplastic and Neoplastic Ground Glass Nodules. *J Inflamm Res*. 2023;16:6155–6166. doi:10.2147/jir.S437419
12. Lee SY, Jeon JH, Jung W, et al. Predictive Factors for Lymph Node Metastasis in Clinical Stage I Part-Solid Lung Adenocarcinoma. *Ann Thorac Surg*. 2021;111(2):456–462. doi:10.1016/j.athoracsur.2020.05.083
13. Travis WD, Brambilla E, Noguchi M, et al. International association for the study of lung cancer/American thoracic society/European respiratory society international multidisciplinary classification of lung adenocarcinoma. *J Thorac Oncol*. 2011;6(2):244–285. doi:10.1097/JTO.0b013e318206a221
14. Moreira AL, Ocampo PSS, Xia Y, et al. A Grading System for Invasive Pulmonary Adenocarcinoma: a Proposal From the International Association for the Study of Lung Cancer Pathology Committee. *J Thorac Oncol*. 2020;15(10):1599–1610. doi:10.1016/j.jtho.2020.06.001
15. Goldstraw P, Chansky K, Crowley J, et al. The IASLC Lung Cancer Staging Project: proposals for Revision of the TNM Stage Groupings in the Forthcoming (Eighth) Edition of the TNM Classification for Lung Cancer. *J Thorac Oncol*. 2016;11(1):39–51. doi:10.1016/j.jtho.2015.09.009
16. Benchoufi M, Matzner-Lober E, Molinari N, Jannot AS, Soyer P. Interobserver agreement issues in radiology. *Diagn Interv Imaging*. 2020;101(10):639–641. doi:10.1016/j.diii.2020.09.001
17. Nitadori J, Bograd AJ, Kadota K, et al. Impact of micropapillary histologic subtype in selecting limited resection vs lobectomy for lung adenocarcinoma of 2cm or smaller. *J Natl Cancer Inst*. 2013;105(16):1212–1220. doi:10.1093/jnci/djt166
18. Ohtaki Y, Yoshida J, Ishii G, et al. Prognostic significance of a solid component in pulmonary adenocarcinoma. *Ann Thorac Surg*. 2011;91(4):1051–1057. doi:10.1016/j.athoracsur.2010.11.071
19. Yeh YC, Kadota K, Nitadori J, et al. International Association for the Study of Lung Cancer/American Thoracic Society/European Respiratory Society classification predicts occult lymph node metastasis in clinically mediastinal node-negative lung adenocarcinoma. *Eur J Cardiothorac Surg*. 2016;49(1):e9–e15. doi:10.1093/ejcts/ezv316
20. Chao L, Yi-Sheng H, Yu C, et al. Relevance of EGFR mutation with micropapillary pattern according to the novel IASLC/ATS/ERS lung adenocarcinoma classification and correlation with prognosis in Chinese patients. *Lung Cancer*. 2014;86(2):164–169. doi:10.1016/j.lungcan.2014.08.018
21. Wang S, Bao X, Yang F, Shi H. Multiparametric evaluation of mediastinal lymph node metastases in clinical T0-T1c stage non-small-cell lung cancers. *Eur J Cardiothorac Surg*. 2024;65(3):59. doi:10.1093/ejcts/ezae059
22. Li W, Zhou F, Wan Z, et al. Clinicopathologic features and lymph node metastatic characteristics in patients with adenocarcinoma manifesting as part-solid nodule exceeding 3 cm in diameter. *Lung Cancer*. 2019;136:37–44. doi:10.1016/j.lungcan.2019.07.029
23. Nelson DB, Godoy MCB, Benveniste MF, et al. Clinicoradiographic Predictors of Aggressive Biology in Lung Cancer With Ground Glass Components. *Ann Thorac Surg*. 2018;106(1):235–241. doi:10.1016/j.athoracsur.2018.02.020
24. He XQ, Li X, Wu Y, et al. Differential Diagnosis of Nonabsorbable Inflammatory and Malignant Subsolid Nodules with a Solid Component ≤5 mm. *J Inflamm Res*. 2022;15:1785–1796. doi:10.2147/jir.S355848

25. Li WJ, Lv FJ, Tan YW, Fu BJ, Chu ZG. Benign and malignant pulmonary part-solid nodules: differentiation via thin-section computed tomography. *Quant Imaging Med Surg*. 2022;12(1):699–710. doi:10.21037/qims-21-145
26. Zhang C, Pang G, Ma C, Wu J, Wang P, Wang K. Preoperative Risk Assessment of Lymph Node Metastasis in cT1 Lung Cancer: a Retrospective Study from Eastern China. *J Immunol Res*. 2019;2019:6263249. doi:10.1155/2019/6263249
27. Qu CH, Li T, Tang ZP, Zhu XR, Han JY, Tian H. Platelet Count is Associated with the Rate of Lymph Node Metastasis in Lung Adenocarcinoma. *Cancer Manag Res*. 2020;12:9765–9774. doi:10.2147/cmar.S273328
28. Chen W, Xu M, Sun Y, et al. Integrative Predictive Models of Computed Tomography Texture Parameters and Hematological Parameters for Lymph Node Metastasis in Lung Adenocarcinomas. *J Comput Assist Tomogr*. 2022;46(2):315–324. doi:10.1097/rct.0000000000001264
29. Xia Y, Li W, Li Y, et al. The clinical value of the changes of peripheral lymphocyte subsets absolute counts in patients with non-small cell lung cancer. *Transl Oncol*. 2020;13(12):100849. doi:10.1016/j.tranon.2020.100849
30. Ettinger DS, Wood DE, Aisner DL, et al. Non-Small Cell Lung Cancer, Version 3.2022, NCCN Clinical Practice Guidelines in Oncology. *J Natl Compr Canc Netw*. 2022;20(5):497–530. doi:10.6004/jnccn.2022.0025
31. Zhang Y, Fu F, Wen Z, et al. Segment Location and Ground Glass Opacity Ratio Reliably Predict Node-Negative Status in Lung Cancer. *Ann Thorac Surg*. 2020;109(4):1061–1068. doi:10.1016/j.athoracsur.2019.10.072
32. Prenzel KL, Mönig SP, Sinning JM, et al. Lymph node size and metastatic infiltration in non-small cell lung cancer. *Chest*. 2003;123(2):463–467. doi:10.1378/chest.123.2.463